Proc. Natl. Acad. Sci. USA
Vol. 93, pp. 1391–1396, February 1996
Cell Biology

A heterotrimeric G protein complex couples the muscarinic m1 receptor to phospholipase C-β

EDGAR DIPPEL*, FRANK KALKBRENNER*, BURGHARDT WITTIG†, AND GÜNTER SCHULTZ*‡

*Institut für Pharmakologie, Freie Universität Berlin, Thielallee 69/73, Federal Republic of Germany; and †Institut für Molekularbiologie und Biochemie, Freie Universität Berlin, Arnimalle 22, D-14195 Berlin, Federal Republic of Germany

Communicated by Lutz Birnbaumer, University of California, Los Angeles, CA, October 24, 1995

ABSTRACT **We addressed the question as to which subtypes of G protein subunits mediate the activation of phospholipase C-β by the muscarinic m1 receptor. We used the rat basophilic leukemia cell line RBL-2H3-hm1 stably transfected with the human muscarinic m1 receptor cDNA. We microinjected antisense oligonucleotides into the nuclei of the cells to inhibit selectively the expression of G protein subunits; 48 hr later muscarinic receptors were activated by carbachol, and the increase in free cytosolic calcium concentration ($[Ca^{2+}]_i$) was measured. Antisense oligonucleotides directed against the mRNA coding for α_q and α_{11} subunits both suppressed the carbachol-induced increase in $[Ca^{2+}]_i$. In cells injected with antisense oligonucleotides directed against α_{o1} and α_{14} subunits, the carbachol effect was unchanged. A corresponding reduction of $G\alpha_q$ and $G\alpha_{11}$ proteins by 70–80% compared to uninjected cells was immunochemically detected 2 days after injection of a mixture of α_q and α_{11} antisense oligonucleotides. Expression of $G\alpha_q$ and $G\alpha_{11}$ completely recovered after 4 days. Cells injected with antisense oligonucleotides directed against the mRNAs encoding for β_1, β_4, and γ_4 subunits showed a suppression of the carbachol-induced increase in $[Ca^{2+}]_i$ compared to uninjected cells measured at the same time from the same coverslip, whereas in cells injected with antisense oligonucleotides directed against the β_2, β_3, γ_1, γ_2, γ_3, γ_5, and γ_7 subunits, no suppression of carbachol effect was observed. In summary, the results from RBL-2H3-hm1 cells indicate that the m1 receptor utilizes a G protein complex composed of the subunits α_q, α_{11}, β_1, β_4, and γ_4 to activate phospholipase C.**

Heterotrimeric guanine nucleotide-binding regulatory proteins (G proteins) functionally couple heptahelical membrane receptors to their effector systems. The G proteins consist of three subunits, α, β, and γ, of which by now 23 α, 5 β, and 11 γ have been identified (for review, see refs. 1–7). They are grouped into four subfamilies, G_s, G_i, G_q, and G_{12}, by homology of their α-subunit sequences. Agonist binding is assumed to induce a conformational change of the receptor, which causes the exchange of GDP for GTP on the G protein α subunit, dissociation of $G\alpha\beta\gamma$ from the activated receptor, and dissociation of the $G\alpha$–GTP from $\beta\gamma$ dimer. Both activated $G\alpha$ and free $G\beta\gamma$ have the capability to interact with different effectors—e.g., adenylyl cyclase, phospholipase C-β (PLC-β), and ion channels. We have shown in a number of different biological systems that receptors selectively use individual α, β, and γ subunits of G proteins in coupling to specific effector systems. In previous studies, we determined the subtypes of the specific G_o proteins coupling muscarinic M_4, somatostatin, and galanin receptors in neuroendocrine cells (i.e., GH_3 and RINm5F) to voltage-gated calcium channels (8–11). Here we determined the subunit composition of the G proteins involved in activation of PLC-β by muscarinic m1 receptors.

The publication costs of this article were defrayed in part by page charge payment. This article must therefore be hereby marked "*advertisement*" in accordance with 18 U.S.C. §1734 solely to indicate this fact.

Muscarinic receptors form a family of five heptahelical receptors (for reviews, see refs. 12 and 13). The muscarinic m1, m3, and m5 receptors stimulate PLC-β via pertussis toxin (PTX)-insensitive G proteins of the G_q family (14, 15), whereas muscarinic m2 and m4 receptors couple to PTX-sensitive $G_{i/o}$ proteins (14, 16). By reconstitution of receptor, G protein, and PLC in phospholipid vesicles, Berstein *et al.* (17) demonstrated that the muscarinic m1 receptor activates PLC-β_1 via purified $G_{q/11}$. In addition, the $G\alpha_q$, $G\alpha_{11}$, and $G\alpha_{14}$ proteins, expressed from recombinant DNAs by the baculovirus–insect cell system, stimulate PLC-β_1 and -β_3 in reconstituted systems (18, 19). The α subunits of the G_q family (α_q, α_{11}, α_{14}, $\alpha_{15/16}$) activate various PLC-β isoforms—i.e., PLC-β_1, -β_3, and -β_4 (20–22)—whereas $\beta\gamma$ dimers activate PLC-β_2 and PLC-β_3 (23–25).

We used rat basophilic leukemia (RBL) cells stably transfected with the m1 muscarinic receptor (RBL-2H3-hm1) as a model system for our studies (26). In these cells stimulation with carbachol, a muscarinic receptor agonist, leads to an increase in inositol phosphates, which in turn releases intracellular Ca^{2+} stores and is followed by Ca^{2+} influx and secretion of serotonin, histamine, and other mediators (26). All these effects are mediated by PTX-insensitive G proteins. To answer the question as to which G protein α subunits are involved in the functional coupling of the muscarinic m1 receptor to PLC-β and whether there are preferential interactions with specific $\beta\gamma$ dimers, we inhibited the expression of G protein subunits by intranuclear microinjection of antisense oligonucleotides complementary to the sequences of the mRNAs of these subunits into RBL-2H3-hm1 cells. The increase in the free cytoplasmic Ca^{2+} concentration ($[Ca^{2+}]_i$) was measured 48 hr later by single-cell imaging of the injected cells loaded with fura-2. Here we provide evidence that a specific complex of heterotrimeric G proteins is involved in the muscarinic m1 receptor-induced increase in $[Ca^{2+}]_i$.

MATERIALS AND METHODS

Materials. PTX was purchased from List Biological Laboratories (Campbell, CA); carbachol, from Sigma; ionomycin and 5′-*N*-ethylcarboxamidoadenosine (NECA), from Calbiochem; L-[*benzilic*-4,4′-^{3}H(N)]quinuclidinyl benzilate ([^{3}H]QNB), from DuPont.

[^{3}H]QNB Binding. RBL cells stably transfected with the muscarinic m1 receptor cDNA (RBL-2H3-hm1) were kindly supplied by P. V. Jones (Burlington, VT) and cultured in medium containing 18% (vol/vol) fetal calf serum (FCS), penicillin at 100 units/ml, and streptomycin at 100 μg/ml. For preparation of membranes, cells were treated as described (27). For estimation of m1 receptor density, binding of

Abbreviations: $[Ca^{2+}]_i$, concentration of free cytoplasmatic calcium; FCS, fetal calf serum; G protein, heterotrimeric guanine nucleotide-binding regulatory protein; PLC, phospholipase C; PTX, pertussis toxin; RBL cells, rat basophilic leukemia cells; RT, reverse transcriptase; NECA, 5′-*N*-ethylcarboxamidoadenosine; [^{3}H]QNB, L-[*benzilic*-4,4′-^{3}H(N)]quinuclidinyl benzilate.

‡To whom reprint requests should be addressed.

[^{3}H]QNB to membranes (25 μg of protein per tube) was performed in a mixture (500 μl) containing 50 mM Tris·HCl (pH 7.5), 5 mM $MgCl_2$, and 1 mM EGTA. Incubation was conducted for 60 min at 37°C. Nonspecific binding was defined as bound [^{3}H]QNB that could not be competed for by 1 μM atropine and was <10%. Separation of membrane-bound and free radioligand was performed by filtration through glass fiber filters (Whatman GF/C) soaked in washing buffer [5 mM $MgCl_2$ and 50 mM Tris·HCl (pH 7.5)] containing 0.33% (vol/vol) polyethyleneimine.

Immunoblotting of G Protein Subunits. Membrane proteins (100 μg) of RBL-2H3-hm1 cells were resolved by SDS/10% PAGE and transferred onto nitrocellulose membranes. Thereafter, to block nonspecific interactions, membranes were incubated for 18 hr at 4°C in PBS (140 mM NaCl, 3 mM KCl, 1.5 mM KH_2PO_4, 8 mM $Na_2HPO_4 \cdot 2H_2O$ at pH 7.4) containing 5% ovalbumin. After washing with PBS, membranes were incubated overnight with either polyclonal rabbit anti-$\alpha_{q/11}$ (AS 370; directed against LQLNLKEYNLV, showing similar properties as the previously published antiserum 368; ref. 28) or anti-$\alpha_{15/16}$ (AS 393; ref. 28) (each diluted 1:100). Then membranes were washed again with PBS and subsequently incubated with peroxidase-conjugated goat anti-rabbit IgG as second antibody (1:2000). Staining was performed with the enhanced chemolumininescence (ECL) Western blotting system (Amersham–Buchler).

Photoaffinity Labeling of RBL-2H3-hm1 Membrane Proteins. Photoaffinity labeling of RBL-2H3-hm1 G proteins, immunoprecipitation, and SDS/PAGE were performed as described (27, 29). For precipitation, 15 μl of antisera specific for $\alpha_{q/11}$ (AS 370) or all three $G\alpha_i$ subunits (AS 266; ref. 30) were used.

Microinjection of Oligonucleotides. RBL-2H3-hm1 cells were seeded at a density of $\approx 10^3$ cells per mm^2 on coverslips imprinted with squares for localization of injected cells. Sequences of all antisense oligonucleotides used in this study were optimized by sequence comparison and multiple alignment using MACMOLLY TETRA software (Soft Gene, Berlin). Oligonucleotides were synthesized with a DNA synthesizer (Milligen model 8600); for synthesis of phosphorothioate oligonucleotides, the method described by Iyer *et al.* (31) was used. Injection of oligonucleotides was performed by a manual injection system (Eppendorf). The injection solution contained 10–20 μM oligonucleotides in water; approximately 10–20 fl was injected with commercially available microcapillaries (Femtotips; Eppendorf) with an outlet diameter of 0.5 μm. The pressure was 20–40 hPa, and the injection time was 0.1 s. After injection, the cells were cultured in culture medium containing 2% FCS for 36 hr; 12 hr before fluorometric measurements, cells were incubated with culture medium containing 18% FCS. The following antisense oligonucleotide sequences were used: anti-α_q, GAACCAATTGTGCATGAGC; anti-α_{11}, CAGGAGTGCATTGGCCTTG; anti-α_{14}, TGGCAGAGTCTGACAGCTG. The sequences of anti-α_{icom} and anti-α_{o1} and of oligonucleotides directed against β and γ subunits have been published (11).

Measurement of Cytosolic Ca^{2+}. RBL-2H3-hm1 cells were loaded with 2 μM fura-2 acetoxymethyl ester (MoBiTec, Göttingen, F.R.G.) for 60 min at 37°C in a buffer consisting of 138 mM NaCl, 6 mM KCl, 0.1 mM $CaCl_2$, 1 mM $MgSO_4$, 1 mM Na_2HPO_4, 5 mM $NaHCO_3$, 5.5 mM glucose, and 20 mM Hepes/NaOH (pH 7.4) containing 0.1% (wt/vol) bovine serum albumin. Cells were washed twice with 2 ml of a buffer consisting of 138 mM NaCl, 6 mM KCl, 1 mM $MgCl_2$, 1 mM $CaCl_2$, 5.5 mM glucose, and 20 mM Hepes/NaOH (pH 7.4). For determination of cytoplasmatic Ca^{2+}, cells were overlayered with 300 μl of the buffer described above, supplemented with 1.1 mM EGTA. Determinations of Ca^{2+} in single cells were performed at 37°C using a digital imaging system (T.I.L.L. Photonics, Munich). Cells were visualized using an inverted microscope (Zeiss Axiovert 100) with a Neofluor ×16 oil-immersion lens (Zeiss). fura-2 fluorescence was excited alternately at 340 nm and 380 nm with illumination provided by a 100-W xenon lamp. Cellular fluorescence was filtered through a 510-nm band pass filter. For each single cell measured, maximum and minimum fluorescence were determined by subsequent addition of the buffer described above containing 10 μM ionomycin plus 2 mM $CaCl_2$ and the same buffer containing 10 mM EGTA, respectively. Images were digitalized and analyzed by the software FUCAL 5.00 (T.I.L.L. Photonics). Ratio images were generated in 0.5- to 1-s intervals. For background compensation, illumination of an area containing no cells was subtracted. For each cell, $[Ca^{2+}]_i$ was averaged from pixels within manually outlined areas. The significance of the results was determined using Student's *t* tests. Standard errors are given as SEM.

Immunocytochemistry. Cells were washed with PBS at pH 7.4, fixed with ethanol/acetic acid (10:1, vol/vol) for 30 min at room temperature, and permeabilized with 0.1% saponine in PBS containing 3% FCS. Then cells were washed (three times, 10 min each) with the same buffer containing 5% FCS and incubated with the same buffer containing 3% FCS with the polyclonal anti-$G_{q/11}$ rabbit antibody (AS 370) at a 1:100 dilution overnight at 4°C. The cells were then washed in PBS (four times, 10 min each) and incubated with goat anti-rabbit IgG conjugated to fluorescein isothiocyanate (diluted 1:1000 or 1:2000) in PBS containing 5% FCS and 0.1% saponine for 18 hr at 4°C. Thereafter, the cells were washed (four times, 10 min each) in PBS and mounted in Moviol (Hoechst). Images of the stained cells were obtained by a video imaging system using monochromatic light at 495 nm at a exposure time of 1000 ms; to prevent bleaching, cells were not exposed to light at 495 nm before pictures were taken. The average of pixels outlined from the immunofluorescence of the cell membrane was corrected for background illumination and was calculated for each cell by constant acquisition parameters. The significance of the results was determined using Student's *t* tests. Standard errors are given as SD. The digitalized fluorescence images were visualized by the software NIH IMAGE (Wayne Rasband, National Institutes of Health).

Reverse Transcriptase (RT)-PCR. Total RNA was purified according to the method of Chomczynski and Sacchi (32), using Trizol (GIBCO/BRL); RT-PCR was performed as described (11). For amplification of $G\alpha_{14}$, primers with the sequences GGAGAAAGAGTCTCAGCGC and TGGCAGAGTCTGACAGCTG were used as primers; for amplification of β and γ subunits, we used the primers reported previously (11).

RESULTS

To study the coupling of m1 receptors to PLC-β, we used RBL-2H3-hm1 cells, which stably express the muscarinic m1 receptor (26), as a model system. Specific binding with [^{3}H]QNB revealed a muscarinic m1 receptor density of 870 fmol/mg of membrane protein (data not shown), which is comparable to the receptor density previously published by Jones *et al.* (26) for these cells; this corresponds to 8500–10,000 receptors per cell.

In this model cell line, carbachol stimulates PLC-β, increases inositol 1,3,4-trisphosphate, and transiently increases $[Ca^{2+}]_i$ by Ca^{2+} release from endoplasmic stores, followed by Ca^{2+} influx. A final event in the signal transduction cascade induced by carbachol in RBL-2H3-hm1 cells is stimulation of serotonin release. All these functional responses were not abrogated by pretreating the cells with PTX (100 ng/ml for 24 hr), which confirms that PTX-insensitive G proteins are mediators between receptor and effector systems (data not shown; ref. 26).

To identify the G protein subunits involved in the m1 receptor-induced increase of $[Ca^{2+}]_i$, we microinjected phos-

phorothioate-modified antisense DNA oligonucleotides directed against the mRNAs of PTX-insensitive and PTX-sensitive G protein α subunits into the nuclei of RBL-2H3-hm1 cells. In experiments studying the persistence of fluorescently labeled antisense oligonucleotides, we detected nuclear fluorescence up to 72 hr after microinjection of oligonucleotides into the nuclei of RBL-2H3-hm1 cells (data not shown).

Two days after injection of antisense oligonucleotides, Ca^{2+} mobilization was measured in the absence of extracellular Ca^{2+} (100 μM EGTA) as an indicator of PLC activation. The increase in $[Ca^{2+}]_i$ was calculated for each cell, and the mean values were calculated for all cells of each experiment as shown in Fig. 1*A* for one typical experiment. The carbachol-induced increase in $[Ca^{2+}]_i$ was largely PTX insensitive (Fig. 1*B*). Cells injected with an antisense oligonucleotide designed to anneal to the mRNAs encoding $G\alpha_q$ (anti-α_q) and $G\alpha_{11}$ (anti-α_{11}) showed largely reduced $[Ca^{2+}]_i$ peaks compared to uninjected cells. Cells injected with antisense oligonucleotides directed against the mRNAs encoding $G\alpha_{o1}$ (anti-α_{o1}) and $G\alpha_{14}$ (anti-α_{14}) subunits were comparable to uninjected cells in showing no reduction in $[Ca^{2+}]_i$ peaks (see Fig. 1*B*). Cells injected with a mixture of anti-α_q and anti-α_{11} antisense oligonucleotides (anti-α_{q+11}) showed no further reduction of carbachol-induced increase in $[Ca^{2+}]_i$ compared to cells injected with either anti-α_q or anti-α_{11} oligonucleotides (see Fig. 1*B*). The expression of members of the G_q family of G proteins in the model cell line was analyzed by probing immunoblots of membranes with specific antisera raised against peptide sequences of $G\alpha_q$, $G\alpha_{11}$, and $G\alpha_{15/16}$. $G\alpha_q$ and $G\alpha_{11}$ proteins were detected; $G\alpha_{15}$ was not expressed (data not shown). In addition, the expression of $G\alpha_{14}$ was demonstrated by RT-PCR using specific $G\alpha_{14}$ primers. To prove the annealing of anti-α_{14} antisense oligonucleotide to the respective cDNA, we used the anti-α_{14} as 3′ primer together with another 5′ primer to amplify nucleotides 29–460 of $G\alpha_{14}$ from cDNA prepared from RBL-2H3-hm1 cells. The specificity of the detected amplified product was tested by restriction analysis (data not shown). These data indicate that m1 receptors couple to both $G\alpha_q$ and $G\alpha_{11}$. To confirm this with a second method, we performed carbachol-stimulated photolabeling with the stable GTP analogue [α-^{32}P]GTP azidoanilide. Immunoprecipitation with a specific anti-$\alpha_{q/11}$ antiserum (AS 370) demonstrated an increased incorporation of [α-^{32}P]GTP azidoanilide into two proteins of 41 and 42 kDa (i.e., G_q and G_{11}); $G\alpha_i$ proteins were not activated by the m1 receptor as shown by immunoprecipitation with an anti-α_{icom} antiserum (AS 266) (data not shown).

To control the specificity of the used antisense oligonucleotides, we compared the m1 receptor-induced increase in $[Ca^{2+}]_i$ with the increase in $[Ca^{2+}]_i$ induced via adenosine A_3 receptors, which are endogenously expressed in RBL-2H3-hm1 cells (33). The adenosine A_3 receptor agonist NECA (10 μM) induced a PTX-sensitive increase in $[Ca^{2+}]_i$ in RBL-2H3-hm1 cells. Since G_{i2} and G_{i3} are the only PTX-sensitive G proteins expressed in this cell line, we injected cells with antisense oligonucleotides complementary to a sequence common to all three mRNAs encoding $G\alpha_i$ isoforms (anti-α_{icom}). On the same coverslip, we injected cells located in another marked area with anti-α_{q+11} antisense oligonucleotides. After application of NECA, anti-α_{icom}-injected cells showed a decreased peak of $[Ca^{2+}]_i$ compared to anti-α_{q+11}-injected cells (Fig. 1 *Inset*), demonstrating the specificity of the antisense oligonucleotides used.

In addition, we checked the ability of the microinjected antisense oligonucleotides to suppress the expression of the targeted G protein subunits, using indirect immunofluorescence. Staining of the G protein subunits α_q and α_{11} in uninjected cells with a specific $G\alpha_{q/11}$ antibody (AS 370) showed a typical ring-shaped pattern of fluorescence, indicating a predominantly plasma membrane-associated location (Fig. 2). Two days after injection of anti-α_{q+11}, the fluorescence signal was reduced by 82% in cells injected with anti-

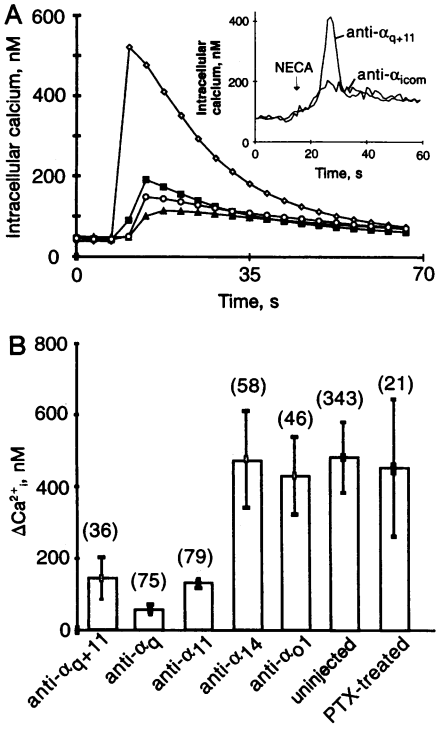

FIG. 1. Carbachol-induced increase in $[Ca^{2+}]_i$ in RBL-2H3-hm1 cells injected with antisense oligonucleotides directed against the mRNAs of $G\alpha_q$, $G\alpha_{11}$, $G\alpha_{14}$, and $G\alpha_{o1}$ in uninjected and PTX-treated cells (100 ng/24 hr). (*A*) The increase in $[Ca^{2+}]_i$ is shown as an average time course for 10–15 cells in representative experiments and determined as described in *Materials and Methods*. ◇, Anti-α_{14}-injected cells; ■, anti-α_{11}-injected cells; ○, anti-α_{q+11}-injected cells; ▲, anti-α_{11}-injected cells. Cells were superfused with carbachol (1 mM) at ≈48 hr after intranuclear injection with the indicated antisense oligonucleotides. (*Inset*) NECA-induced increase in $[Ca^{2+}]_i$ in RBL-2H3-hm1 cells injected with anti-α_{q+11} and anti-α_{icom} antisense oligonucleotides. The arrow indicates the application of NECA (10 μM). (*B*) Bars show mean values (± SEM) of carbachol-induced increase in the intracellular calcium concentration (ΔCa^{2+}). Numbers in parentheses indicate the number of cells measured.

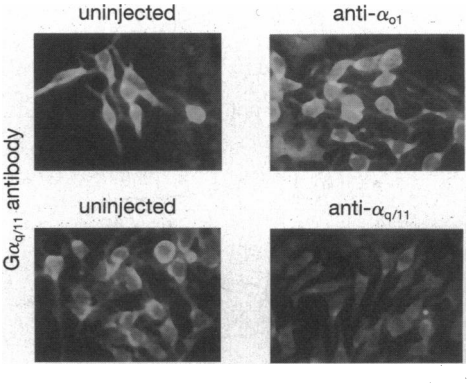

FIG. 2. Inhibition of $G\alpha_{q/11}$ protein expression in RBL-2H3-hm1 cells injected with anti-α_{q+11} antisense oligonucleotides. (*Upper*) Uninjected RBL-2H3-hm1 cells (*Left*) and cells injected with anti-α_{o1} antisense oligonucleotides (*Right*) on the same coverslip. (*Lower*) Uninjected cells (*Left*) and cells injected with anti-α_{q+11} antisense oligonucleotides (*Right*) on the same coverslip. All cells were stained 48 hr after injection with rabbit anti-$\alpha_{q/11}$ antiserum (AS 370; 1:100) specific for $G\alpha_{q/11}$ and visualized by staining with fluorescein isothiocyanate-conjugated goat anti-rabbit IgG (1:1000).

α_{q+11} compared to uninjected cells on the same coverslip (12 ± 10 and 68 ± 30 arbitrary units, respectively). On another coverslip, the fluorescence signal was not significantly different in uninjected compared to control (i.e., anti-α_{o1})-injected cells (88 ± 20 and 110 ± 24 arbitrary units, respectively). The staining patterns in anti-α_{q+11}- and anti-α_{o1}-injected cells were unchanged compared to uninjected cells on the same coverslip (see Fig. 2). The time course of suppression of $G\alpha_{q/11}$ protein expression determined by immunofluorescence microscopy revealed the largest antisense effect (i.e., lowest amount of $G\alpha_{q/11}$ protein expression) 40–48 hr after injection of antisense oligonucleotides. Subunit expression completely recovered 96 hr after injection (data not shown).

Taken together, our data indicate that the muscarinic m1 receptor couples in RBL-2H3-hm1 cells to both $G\alpha_q$ and $G\alpha_{11}$ and that both G proteins are essential to exert its effect on the effector system—i.e., PLC-β.

To identify the β and γ subunits involved in the carbachol-induced increase in $[Ca^{2+}]_i$, we injected antisense oligonucleotides directed against the mRNAs of β_1, β_2, β_3, β_4, γ_1, γ_2, γ_3, γ_4, γ_5, and γ_7 subunits of G proteins (anti-β_1, anti-β_2, anti-β_3, anti-β_4, anti-γ_1, anti-γ_2, anti-γ_3, anti-γ_4, anti-γ_5, and anti-γ_7, respectively). As a stringent control for the specificity of the antisense oligonucleotides, we compared in each experiment injected cells located within a marked area on the coverslip to uninjected cells located outside of the marked area. This procedure guarantees that injected cells were always compared to control cells that were otherwise grown, treated, and analyzed under identical conditions (i.e., incubation, microinjection, loading with fura-2, and determining the increase in $[Ca^{2+}]_i$). Fig. 3 shows the original traces of one experiment. Cells injected with anti-β_1 or anti-β_4 antisense oligonucleotides exhibited a significant inhibition of carbachol-induced increase in $[Ca^{2+}]_i$ compared to uninjected cells, whereas anti-β_2- and anti-β_3-injected cells did not differ from uninjected cells (Figs. 3 and 4*A*). From cells injected with antisense oligonucleotides

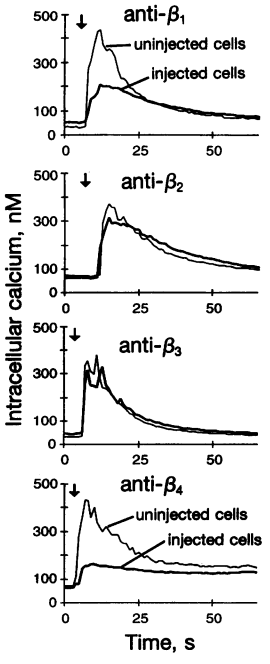

FIG. 3. Carbachol-induced increase in $[Ca^{2+}]_i$ in RBL-2H3-hm1 cells injected with anti-β antisense oligonucleotides. Each panel shows a representative experiment of RBL-2H3-hm1 cells injected with anti-β_1-, anti-β_2-, anti-β_3-, or anti-β_4-injected cells. The tracings show average time courses of about 15 injected and uninjected cells, each measured on the same coverslip. The concentration of $[Ca^{2+}]_i$ was calculated as described in *Materials and Methods.*

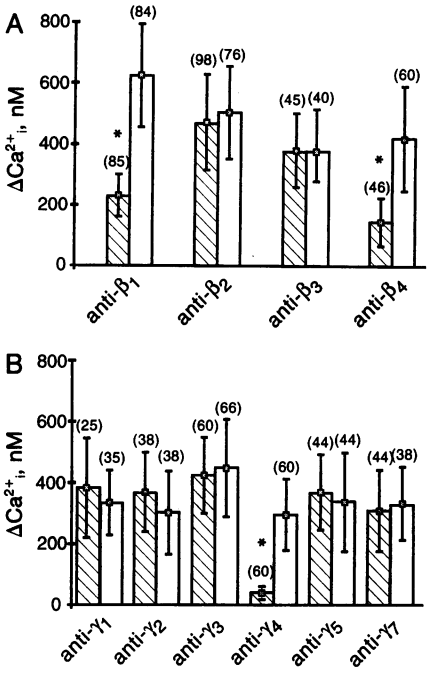

FIG. 4. Carbachol-induced increase in $[Ca^{2+}]_i$ in RBL-2H3-hm1 cells injected with anti-β and anti-γ antisense oligonucleotides. Each bar depicts the carbachol-induced increase in the intracellular calcium concentration ($\Delta Ca^{2+}{}_i$) as the mean ± SEM of seven independent experiments in carbachol-stimulated RBL-2H3-hm1 cells. The numbers of injected and uninjected cells are indicated in parentheses. A nonpaired *t* test was used to assess the significance of the decrease in Ca^{2+} mobilization in antisense oligonucleotide-injected cells compared to uninjected cells (*, $P < 0.01$).

directed against different γ subunits, only anti-γ_4-injected cells showed a strong inhibition of the $[Ca^{2+}]_i$ increase compared to uninjected cells (Fig. 4*B*).

The expression of β and γ subunits was checked by RT-PCR using specific primers for each subunit (11). We found that the β subunits β_1, β_2, β_3, and β_4 were expressed (data not shown). β_5, mainly found in neuronal tissues (34), was not tested. Of the six tested γ subunits, γ_2, γ_3, γ_4, γ_5, and γ_7 were expressed (data not shown). The recently described γ_8 subunit, which is exclusively expressed in olfactory tissue (35), was not tested.

Taken together, our data strongly suggest that the activation of PLC-β and subsequently the induction of $[Ca^{2+}]_i$ increase by m1 receptor are mediated by a G protein complex consisting of the two α subunits, α_q and α_{11}, and two $\beta\gamma$ complexes, $\beta_1\gamma_4$ and $\beta_4\gamma_4$.

DISCUSSION

To study the role of isoforms of G protein subunits in muscarinic m1 receptor–effector coupling in RBL-2H3-hm1 cells *in vivo*, we intranuclearly microinjected antisense oligonucleotides designed to anneal selectively to mRNAs of individual subtypes of G protein subunits. As shown in previous studies, this method guarantees an appropriate molar excess of the antisense oligonucleotides over sense mRNA for effective functional knockouts (8–11). To probe the extent and the selectivity of the antisense knockout effects, we documented the target protein depletion by semiquantitative immunocytochemistry of $G\alpha_{q/11}$. The results of these experiments revealed that the time course by which anti-α_{q+11} antisense oligonucleotides were effective in suppressing functional receptor–PLC-β coupling paralleled suppression of the $G\alpha_{q/11}$ protein level, which decreased maximally within 48 hr after injection. Total recovery of the protein occurred after 96 hr, underlining the reversibility of antisense-induced protein elim-

ination. Similar results were obtained by Kleuss *et al.* (8) using α_{ocom} antisense oligonucleotides in GH_3 cells, by Campbell *et al.* (36) using α_{ocom} and α_{icom} antisense oligonucleotides in dorsal root ganglion cells, and recently by Kalkbrenner *et al.* (11) using specific α_{o1} and α_{o2} antisense oligonucleotides in RINm5F cells.

To prove that targeting of the $\alpha_{q/11}$ subunits by antisense oligonucleotides did not affect other G protein subunits, we compared the carbachol-induced increase in $[Ca^{2+}]_i$ to that induced via the endogenous adenosine A_3 receptor, which couples to PTX-sensitive G proteins. These results demonstrated that injection of anti-α_{q+11} did not affect the functional coupling of the A_3 receptor via G proteins of the G_i family to PLC-β isoforms (see Fig. 1 *Inset*).

The results of our functional studies using microinjection of antisense oligonucleotides showed that in anti-α_q- and anti-α_{11}-injected cells the carbachol-induced $[Ca^{2+}]_i$ increase was substantially suppressed. These data are in agreement with GTP azidoanilide photolabeling experiments demonstrating coupling of the activated m1 receptor, stably transfected in human embryonic kidney 293 cells, primarily to $G\alpha_q$ and $G\alpha_{11}$; in this study the overexpressed m1 receptor also coupled to $G\alpha_{i1}$ and $G\alpha_{i3}$ (27). Similarly, in Chinese hamster ovary (CHO) cells transfected with the m1 receptor, inositol-phospholipid hydrolysis was activated through $G\alpha_{q/11}$ and through PTX-sensitive G proteins (14). In contrast, in RBL-2H3-hm1 cells the m1 receptor coupled only to PTX-insensitive G proteins to activate PLC. One explanation for the fact that we could not observe a PTX-sensitive component of the hormonally stimulated inositol phospholipid response in RBL-2H3-hm1 cells may be due to the number of receptors expressed in these cells, which was more in the range of endogenously expressed receptors compared to other cell lines with overexpressed receptors. In RBL-2H3-hm1 cells, the m1 receptor is expressed at a low density [e.g., 10,000 compared to 350,000 and 140,000 receptors per cell in HEK 293 cells (27) and CHO cells (14), respectively].

Nakamura *et al.* (19) showed that $G\alpha_q$, $G\alpha_{11}$, and $G\alpha_{14}$ proteins expressed in the baculovirus–Sf9 system are equally potent in stimulating purified bovine brain PLC-β in reconstituted systems. Lee *et al.* (37) expressed $G\alpha_q$, $G\alpha_{11}$, $G\alpha_{14}$, and $G\alpha_{16}$ in COS-7 cells and tested the ability of G protein-enriched membranes to stimulate purified PLC-β_1 and PLC-β_2. All members of the G_q protein family reconstituted with the PLC-β_1 isoenzyme, but $G\alpha_q$ and $G\alpha_{11}$ were the most efficient, whereas for reconstitution with the PLC-β_2 isoenzyme $G\alpha_{16}$ was the most efficient subunit. Using the antisense technique in RBL-2H3-hm1, we could not show functionally coupling of the m1 receptor to PLC-β through the $G\alpha_{14}$ protein, although $G\alpha_{14}$ is present in these cells; in addition the anti-α_{14} antisense oligonucleotide did anneal to the targeted sequence in RT-PCR experiments (see *Results*).

Injection of oligonucleotides complementary to specific G protein β and γ subunits also reduced the carbachol-induced $[Ca^{2+}]_i$ increase. In cells injected with anti-β_1 and anti-β_4 oligonucleotides, the carbachol-induced $[Ca^{2+}]_i$ increase was significantly diminished compared to control, anti-β_2-, and anti-β_3-injected cells. When antisense oligonucleotides directed against γ subunits were injected, only anti-γ_4-injected cells showed a significant reduction of the carbachol-induced Ca^{2+} peak. Thus, specific $\beta\gamma$ dimers are involved in functional coupling between the muscarinic m1 receptor and G proteins. High selectivity in functional coupling of one given receptor to one particular G protein heterotrimer has previously been shown in the pituitary cell line GH_3 for muscarinic M_4 and somatostatin receptors, which couple to G_o proteins composed of $\alpha_{o1}/\beta_3/\gamma_4$ and $\alpha_{o1}/\beta_1/\gamma_3$, respectively, to inhibit voltage-gated Ca^{2+} channels (10). Furthermore, in GH_3 as in RINmF5 cells, galanin receptors use G proteins composed of $\alpha_{o1}/\beta_2/\gamma_2$ to mediate inhibition of voltage-gated Ca^{2+} channels (11).

Whether this heterotrimer selectivity is due to a specific interaction of receptors and G proteins or whether the selectivity is due to restricted localization of specific G protein heterotrimers and receptors in the plasma membrane remains to be determined. In fact, there is growing support that compartmentalization may be an important principle in G protein-mediated signal transduction (for review, see ref. 38). The $\beta\gamma$ subunits are sequestered in Triton X-100-insoluble fractions together with cytoskeleton fragments in S49 lymphoma cells (39), and in smooth muscle cells G protein α and β subunits copurify with caveolin, an important structural protein of plasmalemma caveolae (40). Furthermore, the γ_5 subunit in neonatal cardiac fibroblasts is colocalized in focal adhesions with vinculin (41). In addition, the mobility of G protein $\beta\gamma$ subunits is limited in NG108-15 cells (42). Thus, compartmentalization of signaling components hinders free movement of receptors and G proteins in membranes. This may play an important role by determining selectivity in interaction between receptor and effectors. By taking our results into account, one can speculate that receptors may possess structure determinants for specific interaction with G protein heterotrimers or may interact with distinct pools of preformed specific G protein heterotrimers locally enriched in caveolae of cell membranes. For G_q and G_{11}, our data indicate that preformed or precoupled G protein complexes can be composed not only of one heterotrimer but can also consist of two α subunits (α_q and α_{11}), two β subunits (β_1 and β_4), and one γ subunit (γ_4). This complex model is supported by the fact that inhibition of the expression of only one of the involved α subunits leads to abrogation of the functional coupling, what means that each contributes equally to functional coupling. Our data do not exclude that a second, yet unknown, γ subunit participates in m1 receptor–PLC-β coupling, as more γ subunits were recently discovered.

In summary, we show here that specific G proteins composed of $G\alpha_{q/11}\cdot\beta_1/\beta_4\cdot\gamma_4$ are essential for effective coupling between the muscarinic m1 receptor and PLC-mediated Ca^{2+} mobilization in RBL-2H3-hm1 cells. In addition, our approach to use antisense oligonucleotides to identify specific G protein subunits involved in hormonal activation of PLC-β with subsequent increase in cytoplasmatic Ca^{2+} is at present the most suitable and reliable method to determine the specificity of receptor–G protein–effector coupling *in vivo* in intact cells.

We thank Rita Hauboldt for excellent technical assistance, Katrin Büttner for synthesis of oligonucleotides, Karl-Ludwig Laugwitz for help with photolabeling experiments, Dr. Karsten Spicher for providing antisera (especially for the unpublished AS 370), and Dr. Penelope Jones for providing the RBL-2H3-hm1 cells. E.D. was a recipient of a fellowship from the Deutsche Forschungsgemeinschaft. This work was supported by grants from the Deutsche Forschungsgemeinschaft and Fonds der Chemischen Industrie.

1. Simon, M. I., Strathmann, M. P. & Gautam, N. (1991) *Science* **252,** 802–808.
2. Birnbaumer, L. (1992) *Cell* **71,** 1069–1072.
3. Offermanns, S. & Schultz, G. (1994) *Naunyn-Schmiedeberg's Arch. Pharmacol.* **350,** 329–338.
4. Birnbaumer, L. & Birnbaumer, M. (1995) *J. Recept. Signal Transduct. Res.* **15,** 213–252.
5. Neer, E. J. (1995) *Cell* **80,** 249–257.
6. Milligan, G. (1995) *Adv. Pharmacol.* **32,** 1–28.
7. Nürnberg, B., Gudermann, T. & Schultz, G. (1995) *J. Mol. Med.* **73,** 123–132.
8. Kleuss, C., Hescheler, J., Ewel, C., Rosenthal, W., Schultz, G. & Wittig, B. (1991) *Nature (London)* **353,** 43–48.
9. Kleuss, C., Scherübl, H., Hescheler, J., Schultz, G. & Wittig, B. (1992) *Nature (London)* **358,** 424–426.
10. Kleuss, C., Scherübl, H., Hescheler, J., Schultz, G. & Wittig, B. (1993) *Science* **259,** 832–834.

11. Kalkbrenner, F., Degtiar, V. E., Schenker, M., Brendel, S., Zobel, A., Hescheler, J., Wittig, B. & Schultz, G. (1995) *EMBO J.* **14,** 4728–4737.
12. Caulfield, M. P. (1993) *Pharmacol. Ther.* **58,** 319–379.
13. Wess, J., Blin, N., Mutschler, E. & Blüml, K. (1995) *Life Sci.* **56,** 915–922.
14. Ashkenazi, A., Peralta, E. G., Winslow, J. W., Ramachandran, J. & Capon, D. J. (1989) *Cell* **56,** 487–493.
15. Liao, C.-F., Schilling, W. P., Birnbaumer, M. & Birnbaumer, L. (1990) *J. Biol. Chem.* **265,** 11273–11284.
16. Ashkenazi, A. E. G., Winslow, J. W., Peralta, E. G., Peterson, G. L., Schimerlik, M. I., Capon, D. J. & Ramachandran, J. (1987) *Science* **238,** 672–675.
17. Berstein, G., Blanks, J. L., Smrcka, A. V., Higashijima, T., Sternweis, P. C., Exton, J. H. & Ross, E. M. (1992) *J. Biol. Chem.* **267,** 8081–8088.
18. Hepler, J. R., Kozasa, T., Smrcka, A. V., Simon, M. I., Rhee, S. G., Sternweis, P. C. & Gilman, A. G. (1993) *J. Biol. Chem.* **19,** 14267–14375.
19. Nakamura, F., Kato, M., Kameyama, K., Nukada, T., Haga, T., Kato, H., Takenawa, T. & Kikkawa, U. (1995) *J. Biol. Chem.* **270,** 6246–6253.
20. Jhon, D.-Y., Lee, H.-H., Park, D., Lee, C.-W., Lee, K.-H., Yoo, O. J. & Rhee, S. G. (1993) *J. Biol. Chem.* **268,** 6654–6661.
21. Kozasa, T., Hepler, J. R., Smrcka, A. V., Simon, M. I., Rhee, S. G., Sternweis, P. C. & Gilman, A. G. (1993) *Proc. Natl. Acad. Sci. USA* **90,** 9176–9180.
22. Jiang, H., Wu, D. & Simon, M. I. (1994) *J. Biol. Chem.* **269,** 7593–7596.
23. Camps, M., Carozzi, A., Schnabel, P., Scheer, A., Parker, P. & Gierschik, P. (1992) *Nature (London)* **360,** 684–686.
24. Katz, A., Wu, D. & Simon, M. I. (1992) *Nature (London)* **360,** 686–689.
25. Park, D., Jhon, D.-J., Lee, C.-L., Lee, K.-H. & Rhee, S. G. (1992) *J. Biol. Chem.* **268,** 4573–4576.
26. Jones, S. V., Choi, O. H. & Beaven, M. A. (1991) *FEBS Lett.* **289,** 47–50.
27. Offermanns, S., Wieland, T., Homann, D., Sandmann, J., Bombien, E., Spicher, K., Schultz, G. & Jakobs, K. H. (1994) *Mol. Pharmacol.* **45,** 890–898.
28. Spicher, K., Kalkbrenner, F., Zobel, A., Harhammer, R., Nürnberg, B., Söling, A. & Schultz, G. (1994) *Biochem. Biophys. Res. Commun.* **175,** 473–479.
29. Offermanns, S., Schultz, G. & Rosenthal, W. (1991) *Methods Enzymol.* **195,** 286–301.
30. Schmidt, A., Hescheler, J., Offermanns, S., Spicher, K., Hinsch, K.-D., Klinz, F.-J., Codina, J., Birnbaumer, L., Gausepohl, H., Frank, R., Schultz, G. & Rosenthal, W. (1991) *J. Biol. Chem.* **266,** 18025–18033.
31. Iyer, R. P., Egan, W., Regan, J. B. & Beaucage, S. L. (1990) *J. Am. Chem. Soc.* **112,** 1253–1254.
32. Chomczynski, P. & Sacchi, N. (1987) *Anal. Biochem.* **162,** 156–159.
33. Ramkumar, V., Stiles, G. L., Beaven, M. A. & Ali, H. (1993) *J. Biol. Chem.* **268,** 16887–16890.
34. Watson, A. J., Katz, A. & Simon, M. I. (1994) *J. Biol. Chem.* **269,** 22150–22156.
35. Ryba, N. J. P. & Tirindelli, R. (1995) *J. Biol. Chem.* **270,** 6757–6767.
36. Campbell, V., Berrow, N. & Dolphin, A. (1991) *J. Physiol. (London)* **470,** 1–11.
37. Lee, C. H., Park, D., Wu, D., Rhee, S. G. & Simon, M. I. (1992) *J. Biol. Chem.* **267,** 16044–16047.
38. Neubig, R. R. (1994) *FASEB J.* **8,** 939–946.
39. Sargiacomo, M., Sudol, M., Tang, L.-Z. & Lisanti, M. P. (1993) *J. Cell Biol.* **122,** 789–807.
40. Chang, W.-J., Ying, Y.-S., Rothberg, K. G., Hooper, N. M., Turner, A. J., Gambiel, H. A., DeGunzburg, J., Mumby, S. M., Gilman, A. G. & Anderson, R. G. W. (1994) *J. Cell Biol.* **126,** 127–138.
41. Hansen, C. A., Schoering, A. G., Carey, D. J. & Robishaw, J. D. (1994) *J. Cell Biol.* **126,** 811–819.
42. Kwon, G., Axelrod, D. & Neubig, R. R. (1994) *Cell. Signalling* **6,** 663–679.